molecular pharmaceutics

ARTICLE

pubs.acs.org/molecularpharmaceutics

^{99m}Technetium-HYNIC(tricine/TPPTS)-Aca-Bombesin(7−14) as a Targeted Imaging Agent with MicroSPECT in a PC-3 Prostate Cancer Xenograft Model

Hildo J. K. Ananias,[*,†] Zilin Yu,[‡] Rudi A. Dierckx,[‡] Christophe van der Wiele,[§] Wijnand Helfrich,[∥] Fan Wang,[⊥] Yongjun Yan,[#] Xiaoyuan Chen,[#] Igle J. de Jong,[†] and Philip H. Elsinga[‡]

[†]Department of Urology, University Medical Center Groningen, Groningen, The Netherlands

[‡]Department of Nuclear Medicine and Molecular Imaging, University Medical Center Groningen, Groningen, The Netherlands

[§]Department of Nuclear Medicine, University Hospital Ghent, Ghent, Belgium

[∥]Surgical Research Laboratory, University Medical Center Groningen, Groningen, The Netherlands

[⊥]Medical Isotopes Research Center, Peking University, Peking, China

[#]Laboratory of Molecular Imaging and Nanomedicine, National Institute of Biomedical Imaging and Bioengineering, National Institutes of Health, Bethesda, Maryland, United States

ABSTRACT: The peptide bombesin (BN) and derivates thereof show high binding affinity for the gastrin-releasing peptide receptor (GRPR), which is highly expressed in primary and metastasized prostate cancer. We have synthesized a new BN-based radiopharmaceutical ^{99m}technetium-HYNIC(tricine/TPPTS)-Aca-BN(7−14) (^{99m}Tc-HABN) and evaluated its GRPR targeting properties *in vitro* and in a xenograft tumor model for human prostate cancer in athymic mice. ^{99m}Tc-HABN was synthesized, and its lipophilicity and stability were investigated. The IC_{50}, internalization and efflux properties were determined *in vitro* using the GRPR expressing human prostate cancer cell line PC-3. ^{99m}Tc-HABN biodistribution and microSPECT imaging were performed in PC-3 tumor-bearing athymic mice. ^{99m}Tc-HABN was prepared with high labeling yield (>90%), high radiochemical purity (>95%) and a specific activity of ∼19.8 MBq/nmol. The partition coefficient log *D* value was −1.60 ± 0.06. ^{99m}Tc-HABN proved to be stable in human serum for 6 h. The IC50 of HYNIC-Aca-BN(7−14) was 12.81 ± 0.14 nM. Incubation of PC-3 cells with ^{99m}Tc-HABN demonstrated rapid cellular internalization and a long intracellular retention time. When mice were injected with ^{99m}Tc-HABN, the activity was predominantly cleared via the kidneys. Uptake in the tumor was 2.24 ± 0.64% ID/g after 30 min, with a steady decrease during the 4 h study period. *In vivo* experiments with a blocking agent showed GRPR mediated uptake. ^{99m}Tc-HABN microSPECT imaging resulted in clear delineation of the tumor. ^{99m}Tc-HABN is a novel BN-based radiopharmaceutical that proved to be suitable for targeted imaging of prostate cancer with microSPECT using the human prostate cancer cell line PC-3 in a xenograft mouse model.

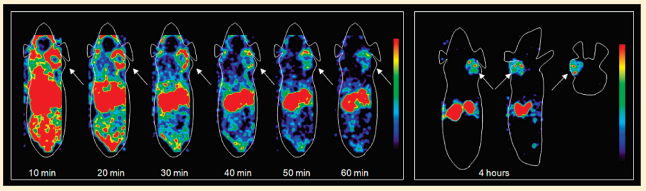

KEYWORDS: bombesin, prostate, cancer, imaging, SPECT, microSPECT, GRPR, GRP

INTRODUCTION

Worldwide, prostate cancer is one of the most common causes of cancer in men and a common cause of morbidity and death.[1,2] As current conventional diagnostic techniques are not sensitive enough to accurately detect early, advanced or recurrent prostate cancer, new diagnostic modalities have to be developed.[3−5] Radionuclide imaging with SPECT or PET (single photon emission computed tomography and positron emission tomography, respectively) may provide a sensitive technique for reliable diagnosis and/or staging of prostate cancer. However, current radiopharmaceuticals appear to have drawbacks with regard to sensitivity or specificity in prostate cancer assessment.[6−8] Crucial for accurate new radionuclide imaging techniques is the development of radiopharmaceuticals that can be targeted to tumor-associated specific antigens, which are overexpressed in prostate cancer and sparse in normal tissue.

In this respect the gastrin-releasing peptide receptor (GRPR) appears to be particularly appealing since it is overexpressed in a variety of human malignancies including primary and metastatic prostate cancer.[9−12] Importantly, GRPR expression in normal tissue is relatively low.[13−16] The natural ligand for GRPR in mammals is the gastrin-releasing peptide (GRP). GRP is not suitable for modification into a radiopharmaceutical since it has poor *in vivo* stability. The amphibian counterpart of GRP, the 14 amino acid peptide bombesin (BN), appeared to be more suitable. GRP and BN share an identical 7 amino acid long C-terminal region that is needed for binding to GRPR. A series of

Received: January 12, 2011
Accepted: June 23, 2011
Revised: May 6, 2011
Published: June 23, 2011

dx.doi.org/10.1021/mp200014h | *Mol. Pharmaceutics* 2011, 8, 1165–1173

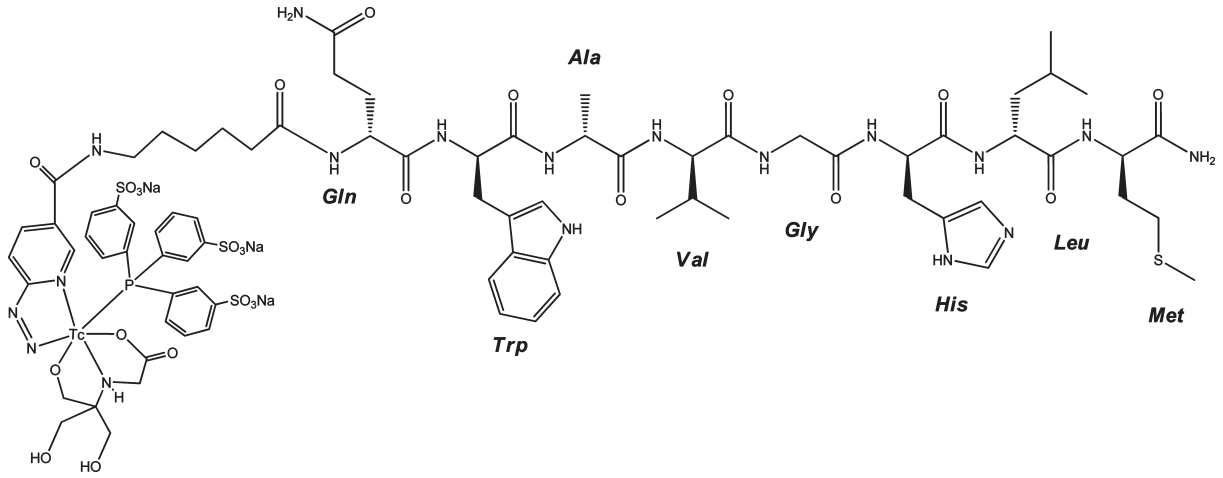

Figure 1. ^{99m}Tc-HYNIC(tricine/TPPTS)-Aca-BN(7−14). Note: coordination of the ternary ligand complex to ^{99m}Tc according to Surfraz et al.[53].

BN analogues have been constructed that were labeled with a variety of radionuclides (i.e., ^{99m}Tc, ^{111}In, ^{64}Cu, ^{18}F).[17] Several groups have used either the full length BN molecule, BN(1−14), or the truncated peptide BN(7−14), with or without amino acid substitutions, spacer insertion and different radionuclide−chelator complexes in order to achieve increased affinity for GRPR, higher metabolic stability, improved biodistribution properties or manipulation of the mode of excretion.

Although radiolabeled BN derivatives have been extensively investigated for diagnosis and treatment of GRPR positive prostate tumors in preclinical studies,[17−19] clinical research in prostate cancer patients is limited to only a few compounds.[20−24] For that reason, in this study we investigated the efficacy of a novel BN-based radiopharmaceutical in a human prostate cancer xenograft mouse model as a prelude to clinical evaluation.

Therefore, we synthesized a novel radiopharmaceutical composed of the truncated BN peptide BN(7−14) which was conjugated to the bifunctional coupling agent 6-hydrazinonicotinic acid (HYNIC) linked by ε-aminocaproic acid (Aca) that was used as a spacer. With the coligands tricine and trisodium triphenylphosphine-3,3′,3″-trisulfonate (TPPTS), the HYNIC/tricine/TPPTS complex was used for ^{99m}Tc labeling and to form ^{99m}Tc-HYNIC(tricine/TPPTS)-Aca-BN(7−14) (^{99m}Tc-HABN, Figure 1). The ternary ligand system was chosen because of its high labeling efficiency (rapid and high yield radiolabeling), high stability, relatively easy use and hydrophilicity.[25] The HYNIC-(tricine/TPPTS) complex has been successfully used for radiolabeling peptides and receptor antagonists.[26−31]

The main objective of the current study is to preclinically evaluate the suitability of the novel radiopharmaceutical ^{99m}Tc-HABN as a targeted imaging agent of prostate cancer using the human prostate cancer cell line PC-3 in a xenograft mouse model.

EXPERIMENTAL SECTION

Chemicals. Tricine (*N*-(tri(hydroxymethyl)methyl)glycine) and Aca-BN(1−14) were purchased from Sigma/Aldrich (St. Louis, MO, USA), and TPPTS was purchased from Alfa Aesar (Karlsruhe, Germany). Both were used without further purification. The peptide conjugate Aca-BN(7−14) was acquired as described previously.[32] HYNIC-Aca-BN(7−14) was synthesized as described below. Na^{99m}TcO$_4$ was produced according to standard procedures using the ^{99} Mo/^{99m}Tc generator in our department. ^{125}I-Tyr^4-BN was obtained from Perkin-Elmer Life and Analytical Sciences (Waltham, MA, USA).

Equipment. Analytical as well as semipreparative reversed-phase high-performance liquid chromatography (RP-HPLC) was performed on a HITACHI L-2130 HPLC system (Hitachi High Technologies America Inc., Pleasanton, CA, USA) equipped with a Bicron Frisk-Tech area monitor. Isolation of radiolabeled peptides was performed using a Phenomenex reversed-phase Luna C18 column (10 mm × 250 mm, 5 μm) (Torrance, CA, USA). The flow was set at 2.5 mL/min using a gradient system starting from 90% solvent A (0.01 M phosphate buffer, pH = 6.0) and 10% solvent B (acetonitrile) (5 min) and ramped to 45% solvent A and 55% solvent B at 35 min. The analytic HPLC was performed using the same gradient system but with a reversed-phase Grace Smart RP-C18 column (Lokeren, Belgium) (4.6 mm × 250 mm, 5 μm) and a flow of 1 mL/min.

Synthesis of HYNIC-Aca-Bombesin(7−14). HYNIC-Boc (16.7 mg; 47.5 μmol) (Boc = *tert*-butyloxycarbonyl) and BN-(7−14) (50 mg; 47.5 μmol) were dissolved in 0.3 mL of *N*,*N*-dimethylformamide. 30 μL of *N*,*N*-diisopropylethylamine was then added, and the mixture was vortexed for 1 min. The reaction was complete after 2 h, and no degradation products of HYNIC-Aca-BN(7−14) were found in the final product. 40 μL of acetic acid was added to quench the reaction. The crude product was subjected to HPLC purification. The desired fraction was collected and lyophilized. Anhydrous trifluoroacetic acid (2 mL) was then added to remove the protecting Boc group. After 20 min, the trifluoroacetic acid solution was blown dry. The crude HYNIC-Aca-BN(7−14) was purified by HPLC and lyophilized. Product identity was confirmed by MALDI-TOF MS (matrix-assisted laser desorption/ionization time-of-flight mass spectrometry): m/z 1188.29 for $[MH]^+$ ($C_{55}H_{81}N_{17}O_{11}S$) calculated molecular weight: 1187.60. Pure product was stored in a −20 °C freezer.

Radiochemistry. Twenty microliters of the HYNIC-Aca-BN-(7−14) solution (1 mg/mL in H_2O), 100 μL of tricine solution (100 mg/mL in 25 mM succinate buffer, pH 5.0), 10 μL of $SnCl_2$ solution (3.0 mg/mL in 0.1 N HCl) and 100 μL of Na^{99m}TcO$_4$ (370 MBq) in saline were added to a 1.5 mL Eppendorf vial. The reaction mixture was kept at 95 °C for 5 min. 100 μL of the TPPTS solution (50 mg/mL in 25 mM succinate buffer, pH 5.0) was added to the reaction mixture. The Eppendorf vial containing the reaction mixture was sealed and heated at 95 °C for

20 min. After cooling to room temperature, the mixture was purified by semipreparative HPLC. The product was then passed through a Sep-Pak C-18 cartridge. The Sep-Pak C-18 cartridge was activated with ethanol (10 mL) and was washed with water (10 mL) before use. After the product was loaded, the Sep-Pak C-18 cartridge was washed with saline (10 mL). The radiotracer was eluted with 70% ethanol (0.4 mL) for *in vitro* and *in vivo* experiments. A sample of the resulting solution was analyzed by radio-HPLC.

Partition Coefficient. The partition coefficient was determined using the method described previously.[29] The tracer was dissolved in a mixture of 0.5 mL of *n*-octanol and 0.5 mL of 25 mM phosphate buffer (pH 7.4) and well mixed. Then the mixture was centrifuged at 3000 rpm for 5 min. 100 μL samples were obtained from *n*-octanol and aqueous layers and were counted in a γ-counter (Compugamma CS1282, LKB-Wallac, Turku, Finland). The log *D* value is reported as an average of three different measurements.

***In Vitro* Stability.** ^{99m}Tc-HABN was dissolved in 1 mL of saline or cysteine solution (1 mg/mL), incubated at room temperature and analyzed by RP-HPLC at 1, 2, 4, 6, and 24 h post incubation.

The study of metabolic stability was performed in human serum. Human serum from healthy donors was incubated at 37 °C with ^{99m}Tc-HABN for different time periods (1, 2, 4, 6, 24 h). After incubation, a sample of 250 μL was precipitated with 750 μL acetonitrile/ethanol ($V_{acetonitrile}/V_{ethanol}$ =1:1) and then centrifuged (3 min at 3000 rpm), the supernatants were passed through a filter and afterward analyzed by RP-HPLC. Results were plotted as the radiochemical purity (RCP) at different time points.

Dose Preparation for Animal Studies. Doses for animal studies were prepared by dissolving the Sep-Pak C18 cartridge purified radiotracer in saline to give a concentration of 5.6 MBq/mL (~0.56 MBq/mouse, ethanol concentration ~0.1%) for the biodistribution study and 300 MBq/mL (~60 MBq/mouse, ethanol concentration ~10%) for the imaging study.

Cell Culture. The GRPR positive PC-3 human prostate cancer cell line (ATCC, Manassas, VA, USA) was cultured in RPMI 1640 (Lonza, Verviers, France) supplemented with 10% fetal calf serum (Thermo Fisher Scientific Inc., Logan, UT, USA) at 37 °C in a humidified 5% CO_2 atmosphere.

***In Vitro* Competitive Receptor Binding Assay.** The *in vitro* GRPR binding affinities of Aca-BN(7−14) and HYNIC-Aca-BN(7−14) were compared to BN(1−14) and assessed via a competitive displacement assay with ^{125}I-Tyr^4-BN(1−14) as the GRPR specific radioligand. Experiments were performed at 37 °C with PC-3 human prostate cancer cells according to a method previously described.[33] The 50% inhibitory concentration (IC_{50}) values were calculated by fitting the data with nonlinear regression using GraphPad Prism 5.0 (GraphPad Software, San Diego, CA, USA). Experiments were performed with triplicate samples. IC_{50} values are reported as an average of these samples plus the standard deviation (SD).

Internalization Studies. One day prior to the assay, PC-3 cells were seeded in 6-well plates. The 6-well plates were then incubated with ^{99m}Tc-HABN (0.0037 MBq/well) for 2 h at 4 °C. To remove unbound radioactivity, the cells were washed twice afterward with ice-cold PBS and were then incubated in the prewarmed culture medium at 37 °C for 0, 5, 15, 30, 45, 60, 90, and 120 min in triplicate to allow for internalization.

To remove cell-surface bound ^{99m}Tc-HABN, the cells were washed twice for 3 min with acid (50 mM glycine−HCl/100 mM NaCl, pH 2.8). Next, the cells were lysed by incubation with 1 M NaOH at 37 °C and the resulting lysate in each well was aspirated to determine the internalized radioactivity in a γ-counter (Compugamma CS1282, LKB-Wallac, Turku, Finland). Results are expressed as the percentage of total radioactivity (internalized activity/(surface-bound activity + internalized activity)) (mean ± SD).

Efflux Studies. One day prior to the assay, PC-3 cells were seeded in 6-well plates. The 6-well plates were then incubated with ^{99m}Tc-HABN (0.0037 MBq/well) for 1 h at 37 °C to allow for internalization. To remove unbound radioactivity, the cells were washed twice afterward with cold (0 °C) PBS and were then incubated using prewarmed culture medium (37 °C) for 0, 15, 30, 45, 60, 90, 120, and 240 min in triplicate to allow for externalization. To remove cell-surface bound ^{99m}Tc-HABN, the cells were washed twice for 3 min with acid (50 mM glycine−HCl/100 mM NaCl, pH 2.8). Next, the cells were lysed by incubation with 1 M NaOH at 37 °C, and the resulting lysate in each well was aspirated to determine the remaining radioactivity in a γ-counter (Compugamma CS1282, LKB-Wallac, Turku, Finland). Results are expressed as the percentage of maximum intracellular radioactivity (remaining activity at specific time-point/activity at time point 0) (mean ± SD).

Animal Model. The xenograft tumor model for human prostate cancer in athymic mice was generated by subcutaneous injection of 2×10^6 PC-3 cells (suspended in 0.1 mL of sterile saline) in the right front flank of male athymic mice (Harlan, Zeist, The Netherlands). During the injection, animals were anesthetized with a gas composed of ~3.5% isoflurane in an air/oxygen mixture. The mice were used for biodistribution experiments and micro-SPECT imaging when the tumor volume reached a mean diameter of ~0.8−1.0 cm (3−4 weeks after inoculation).

All animal experiments were performed in accordance with the regulations of Dutch law on animal welfare and the institutional ethics committee for animal procedures approved the protocol.

Biodistribution Experiments. Twelve PC-3 tumor-bearing mice were randomly divided into three groups of four animals. Isoflurane inhalation was used as method of anesthesia. ^{99m}Tc-HABN (~0.56 MBq/mouse) dissolved in 0.1 mL of saline was injected intravenously via the penis vein. At time points 0.5, 1, and 4 h postinjection (p.i.), the mice were anesthetized again and sacrificed by cervical dislocation. Immediately after sacrifice, blood samples were withdrawn from the retro orbital sinus using capillary tubes, and organs of interest (heart, liver, spleen, lung, kidney, pancreas, small intestine, large intestine, stomach, bone, muscle and tumor) were collected and wet weighed. Radioactivity was determined in a γ-counter (Compugamma CS1282, LKB-Wallac, Turku, Finland).

To determine specificity of the *in vivo* uptake of ^{99m}Tc-HABN, a fourth group of 4 mice received an intravenous injection of 300 μg of unlabeled HYNIC-Aca-BN(7−14) (in 0.2 mL of saline) as blocking agent 30 min prior to injection of ^{99m}Tc-HABN (~0.56 MBq/mouse in 0.1 mL). The mice were sacrificed 1 h after injection of the radiotracer. Blood and organs were collected, weighed and counted as described above.

Organ and tissue uptake was calculated as a percentage of the injected dose per gram of tissue mass (% ID/g). Biodistribution data is reported as an average plus the SD based on the results from four animals at each time point. Significant blocking was calculated with the Student's *t* test. *P*-values are considered significant when $p \leq 0.05$. Tumor-to-normal-tissue (T/NT) ratios are reported as an average at each time point (without the blocking group).

MicroSPECT Imaging. The imaging study was performed in seven PC-3 tumor-bearing mice, of which four were used for

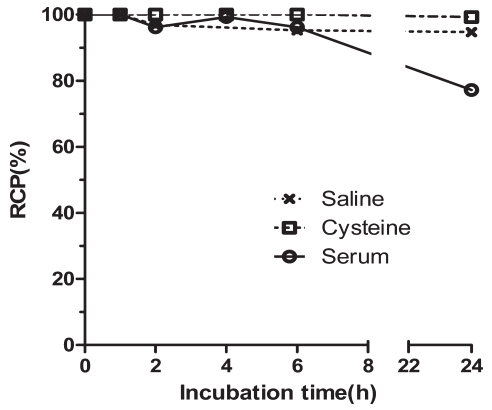

Figure 2. *In vitro* stability of ^{99m}Tc-HYNIC(tricine/TPPTS)-Aca-BN-(7−14). Results are plotted as the RCP at different time points.

^{99m}Tc-HABN imaging and three were used for the blocking experiment. Each PC-3 tumor-bearing mouse was penis vein injected with ^{99m}Tc-HABN (∼60 MBq/mouse) in 0.2 mL of saline using isoflurane anesthesia. Animals were placed prone on a three-head γ-camera (MILabs, U-SPECT-II, Utrecht, The Netherlands) equipped with a multipinhole high-resolution collimator (diameter 0.6 mm, resolution about 0.4 mm). Immediately after injection of the radiotracer, dynamic data was acquired for 1 h (6 frames, 10 min per frame). The mice were sacrificed 4 h after injection of the radiotracer and placed prone in the U-SPECT-II, and a static scan was performed for 1 h. The imaging data was stored digitally in list mode.

For the blocking experiment, excess cold HYNIC-Aca-BN-(7−14) (300 μg dissolved in 0.2 mL of saline) was administered intravenously via the penis vein in three mice 30 min prior to administration of ^{99m}Tc-HABN(∼60 MBq/mouse). Data was acquired using the same procedure as described above.

Images were reconstructed by using U-SPECT-Rec v 1.34i3 (MILabs, Utrecht, The Netherlands) with a pixel-based ordered-subsets expectation maximum (POSEM) algorithm. Final images were 1 mm slices, made with Amide 0.9.1 (open source software).

Radioactivity accumulation in tumor was quantified with the use of Amide 0.9.1 by drawing regions of interest (ROI) around the tumor on U-SPECT images of PC-3 tumor bearing mice at 10, 20, 30, 40, 50, 60, and 240 min postinjection of ^{99m}Tc-HABN, preinjected with or without excess blocking agent. ROI values were corrected for the injected dose (final ROI = ROI calculated with Amide software divided by the injected dose) and expressed as mean ± SD. Significant blocking was calculated with the Student's *t* test.

RESULTS

Synthesis, Radiolabeling, Partition Coefficient and *In Vitro* Stability. Within 30 min ^{99m}Tc-HABN (Figure 1) was prepared at 95 °C with high labeling yield (>90%) and radiochemical purity after purification (>95%). The specific activity was ∼19.8 MBq/nmol. ^{99m}Tc-HABN was analyzed using a reversed phase HPLC method. The HPLC retention time was 21.5 min for ^{99m}Tc-HABN and 19.5 min for HYNIC-Aca-BN(7−14).

The partition coefficient was determined in a mixture of *n*-octanol and phosphate buffer (pH = 7.4). The log *D* value was −1.60 ± 0.06. The *in vitro* stability of ^{99m}Tc-HABN was tested in saline, in human serum, and in the presence of excess cysteine (1.0 mg/mL, pH = 7.4) (Figure 2). ^{99m}Tc-HABN was stable in the presence of excess cysteine and human serum for at least 6 h. The RCP of ^{99m}Tc-HABN in serum slowly decreased to 77% after 24 h.

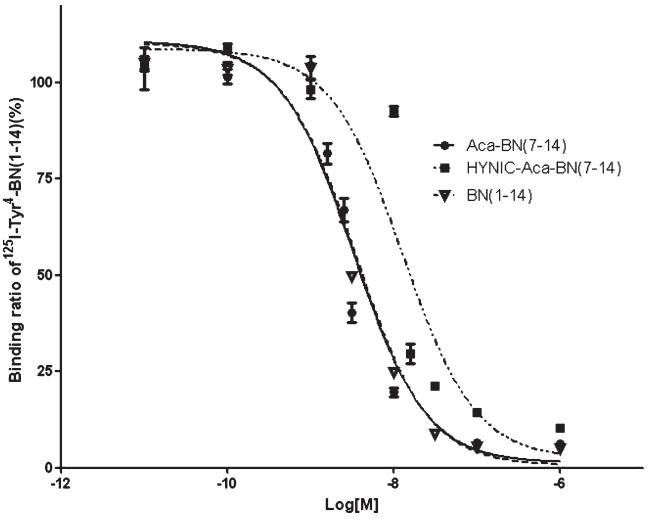

Figure 3. Displacement curve of ^{125}I-Tyr^4-BN(1−14) binding to GRPR on PC-3 cells. Log [M] = log of increasing concentration (mol/L) of Aca-BN(7−14), BN(1−14) and HYNIC-Aca-BN(7−14).

***In Vitro* Competitive Receptor Binding Assay.** Using ^{125}I-Tyr^4-BN(1−14) as the GRPR specific radioligand, the binding affinities of Aca-BN(7−14) and HYNIC-Aca-BN(7−14) for GRPR were compared to BN(1−14), set as the standard, via a competitive displacement assay. Results are plotted in sigmoid curves for the displacement of ^{125}I-Tyr^4-BN(1−14) as a function of increasing concentrations of Aca-BN(7−14), BN(1−14) and HYNIC-Aca-BN(7−14) (Figure 3). The IC_{50} values were found to be 3.27 ± 0.28, 3.48 ± 0.17 and 12.81 ± 1.34 nM for Aca-BN(7−14), BN(1−14) and HYNIC-Aca-BN(7−14), respectively.

Internalization and Efflux Studies. The internalization study depicted in Figure 4A showed rapid internalization of ^{99m}Tc-HABN into PC-3 cells within 5−15 min. Internalization reached a plateau of ∼84% after 30 min, which remained steady for the duration of the experiment (120 min).

Figure 4B shows the efflux kinetics of ^{99m}Tc-HABN. Moderate efflux in the first 60 min was demonstrated with only one-third of the activity externalized by the PC-3 cells. After 90 min a relatively stable situation was created with just over 50% of the internalized radioactivity remaining in the cells for the remainder of the experiment. The $t_{1/2}$ efflux of ^{99m}Tc-HABN PC-3 cells was 38 ± 5 min.

Biodistribution Experiments. Biodistribution of ^{99m}Tc-HABN was evaluated in athymic mice bearing PC-3 tumors. Results of the biodistribution, the blocking experiment and T/NT ratios are shown in Table 1.

Uptake in PC-3 tumor and the GRPR rich mouse pancreas[34] was highest (2.24 ± 0.64 and 17.3 ± 1.69% ID/g, respectively) at 30 min p.i., with a steady decrease over the 4 h study period. Uptake in the tumor and pancreas was reduced significantly after injection of the blocking agent, indicating specific GRPR targeting of ^{99m}Tc-HABN. Uptake in other GRPR expressing organs (stomach and intestine) was also significantly reduced in the study of GRPR blockade.

While hepatic uptake was modest, uptake in the kidneys was high and radioactivity was rapidly cleared from the blood via the

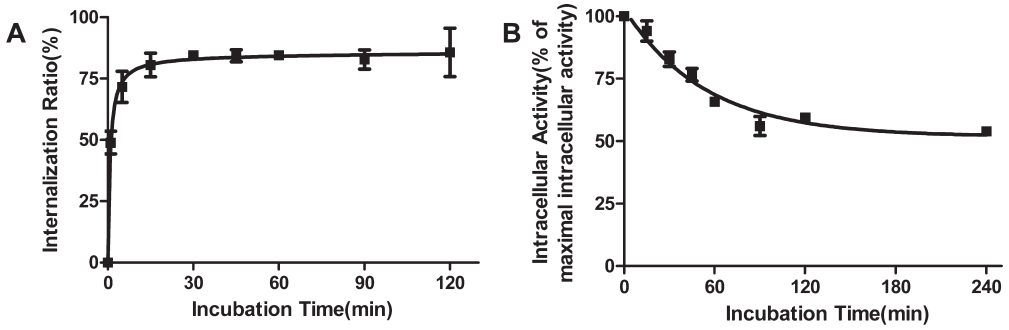

Figure 4. (A) ^{99m}Tc-HYNIC(tricine/TPPTS)-Aca-BN(7−14) internalization experiment. Results are expressed as the percentage of total radioactivity (internalized activity/(surface-bound activity plus internalized activity)) (mean ± SD). (B) ^{99m}Tc-HYNIC(tricine/TPPTS)-Aca-BN(7−14) efflux experiment. Results are expressed as the percentage of maximum intracellular radioactivity (remaining activity at specific time-point divided by activity at time point 0) (mean ± SD).

Table 1. Biodistribution and Tumor-to-Normal-Tissue Ratios of ^{99m}Tc-HABN after Intravenous Injection in PC-3 Prostate Tumor Bearing Athymic Mice[a]

	30 min		1 h		4 h		
organ	% ID/g	T/NT	% ID/g	T/NT	% ID/g	T/NT	1 h + blocking, % ID/g
blood	1.06 ± 0.17	2.12	0.45 ± 0.19	3.66	0.06 ± 0.01	12.69	0.50 ± 0.12
heart	0.35 ± 0.08	6.44	0.17 ± 0.07	9.56	0.04 ± 0.01	18.71	0.18 ± 0.04
liver	1.33 ± 0.20	1.76	0.60 ± 0.11	2.52	0.13 ± 0.03	5.19	0.55 ± 0.16
spleen	0.48 ± 0.08	4.64	0.57 ± 0.54	4.11	0.16 ± 0.08	5.10	0.19 ± 0.04
lung	1.30 ± 0.16	1.77	0.52 ± 0.18	3.11	0.08 ± 0.02	8.27	0.60 ± 0.19
kidney	7.09 ± 4.40	0.71	6.39 ± 0.83	0.24	4.00 ± 0.68	0.16	9.57 ± 5.97
small intestine	6.78 ± 2.24	0.36	4.10 ± 1.60	0.43	1.30 ± 0.79	0.65	1.84 ± 0.94*
large intestine	3.54 ± 1.00	0.67	2.80 ± 0.71	0.55	2.43 ± 0.73	0.31	0.42 ± 0.12*
stomach	2.22 ± 0.31	1.05	1.39 ± 0.38	1.11	0.44 ± 0.15	1.65	0.38 ± 0.12*
bone	0.55 ± 0.46	5.54	0.25 ± 0.11	7.62	0.06 ± 0.02	10.67	0.14 ± 0.05
muscle	0.48 ± 0.35	5.86	0.12 ± 0.04	13.92	0.02 ± 0.01	40.19	0.13 ± 0.04
pancreas	17.3 ± 1.69	0.13	8.92 ± 1.74	0.17	5.02 ± 0.94	0.13	0.34 ± 0.11*
PC-3 tumor	2.24 ± 0.64	1.00	1.51 ± 0.38	1.00	0.67 ± 0.26	1.00	0.47 ± 0.14*

[a] Values are expressed as % ID/g, mean ± standard error of the mean/standard deviation (n = 4 at each time point) or as T/NT ratios. Blocking was achieved by preinjection of 300 μg of unlabeled HYNIC-Aca-BN(7-14); * = statistically significant difference ($p < 0.05$).

preferred renal-urinary route. When an excess of cold HYNIC-Aca-BN(7−14) was injected prior to ^{99m}Tc-HABN injection, nonspecific uptake in the kidneys was increased further, probably as a result of an increased level of circulating unbound ^{99m}Tc-HABN.

Low uptake of radioactivity in bone and muscle, combined with the rapid clearance from the blood pool, resulted in high T/NT ratios, increasing over time.

MicroSPECT Imaging. Figure 5 shows the coronal microSPECT images (sections) acquired with the high resolution U-SPECT-II after injection of ∼60 MBq ^{99m}Tc-HABN with and without the blocking agent in PC-3 tumor bearing mice. The tumor could already be seen 10 min after injection of ^{99m}Tc-HABN, and tumor-to-background contrast increased over the first hour (Figure 5A), resulting in excellent tumor delineation after 4 h (Figure 5B). Noteworthy, the outer rim of the tumor displayed high uptake of activity while the central part of the tumor shows reduced binding.

Prominent uptake was also seen in the pancreas (not shown) and both kidneys in all time frames. In addition, clearance via the urinary bladder was evident. Preinjection of an excess of the blocking agent reduced uptake in the tumor and other GRPR positive organs considerably, while the kidneys remained visible (Figure 5C,D).

Figure 6 shows the radioactivity accumulation quantification in the tumor from the ^{99m}Tc-HABN U-SPECT images with and without blocking agent. Tumor uptake diminished over time as was determined before in the biodistribution study. Uptake was significantly higher without the preadministration of the blocking agent at all time points, except at 20 and 40 min p.i.

■ DISCUSSION

Current conventional diagnostic techniques are not sensitive enough to accurately detect early advanced or recurrent prostate cancer. Therefore, better diagnostic modalities are urgently needed. We developed a novel BN-based radiopharmaceutical, designated ^{99m}Tc-HABN, and investigated its potency for the *in vitro* and *in vivo* binding to prostate cancer expressed GRPR.

For widespread use of a tracer in clinical practice, a radioisotope with a relatively long half-life, high labeling efficiency and good availability is mandatory. We therefore utilized the popular γ-emitting isotope ^{99m}Tc.[17] The HYNIC/tricine/TPPTS

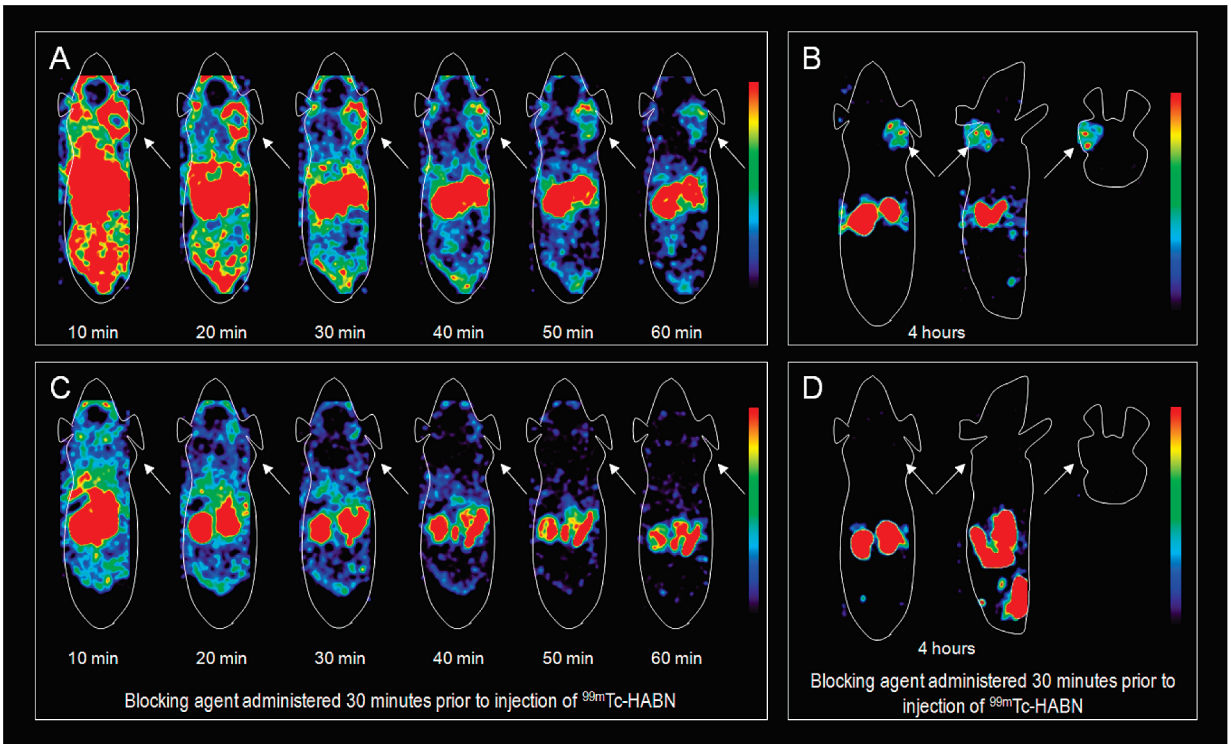

Figure 5. Coronal microSPECT images (sections) at ten minute intervals during the first hour after injection of ^{99m}Tc-HABN without blocking agent (A) and with blocking agent (C). Static coronal, sagittal and axial images (sections) 4 h after injection of ^{99m}Tc-HABN without blocking agent (B) and with blocking agent (D). Arrows indicate the tumor.

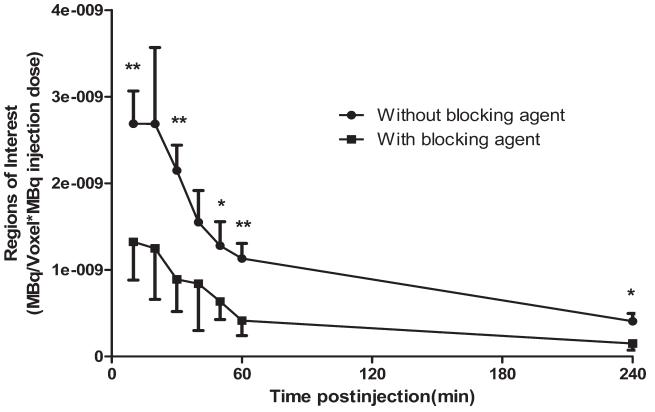

Figure 6. The radioactivity accumulation quantification in tumor from the microSPECT images of PC-3 tumor bearing mice at 10, 20, 30, 40, 50, 60, and 240 min postinjection of ^{99m}Tc-HABN, preinjected with or without excess blocking agent. The ROI values were corrected for the injected dose and expressed as mean ± SD. * = statistically significant difference ($p < 0.05$), ** = statistically significant difference ($p < 0.01$).

complex was used because of its high labeling efficiency (rapid and high yield radiolabeling), high solution stability and relatively easy use.[25] It was also chosen because of its hydrophilic character leading to the preferred excretion route via the renal-urinary system.[26,29,35,36] Shi et al. demonstrated excellent results with HYNIC coupled β-alanine-BN(7−14)[29] *in vitro* in PC-3 prostate cancer cells and *in vivo* in a colon cancer mouse model. By changing β-alanine to Aca we sought to improve GRPR targeting properties and pharmacokinetics both *in vitro* and *in vivo* in a prostate cancer model.

^{99m}Tc-HABN was synthesized with high radiochemical yield and purity. In addition, ^{99m}Tc-HABN proved highly stable in saline, cysteine solution and human serum. *In vitro* experiments revealed that although the addition of HYNIC to Aca-BN-(7−14) reduces the binding affinity for GRPR, the IC_{50} value of HYNIC-Aca-BN(7−14) is still in the nanomolar range (12.8 ± 0.14 nM) and therefore very similar to IC_{50} values reported for other BN derivatives with HYNIC, DOTA or (N^aHis)Ac as chelator.[29,37−43] Internalization into PC-3 cells occurred rapidly, while long retention was seen in the efflux experiments with more than 50% of the internalized radioactivity remaining after 4 h.

Because primary prostate cancer is located in the pelvis and lymph node metastases are situated mainly in the pelvis and abdomen, rapid renal-urinary clearance is generally preferred over hepatoenteric clearance in order to limit pelvicoabdominal background activity as much as possible and thus to achieve good imaging contrast.

In clinical practice, urinary activity in the bladder can be evacuated by micturition prior to the scan or, if needed, by bladder drainage. Determination of the partition coefficient of ^{99m}Tc-HABN demonstrated a hydrophilic compound, which should govern excretion through the kidneys rather than via the liver. This was confirmed by the *in vivo* determination of the biodistribution of ^{99m}Tc-HABN in athymic mice bearing human prostate cancer tumors as uptake in liver was only 1.33 ± 0.20% ID/g after 30 min, while uptake in the kidneys was high after 30 min (7.09 ± 4.40% ID/g) and remained high for 4 h p.i. Preinjection with the blocking agent did not reduce kidney uptake or excretion of ^{99m}Tc-HABN.

Furthermore, *in vivo* biodistribution experiments also showed rapid tumor uptake, being the highest at 30 min p.i. (2.24 ± 0.64% ID/g)

and decreasing slowly over the evaluated period of 4 h. Uptake in tumor is even higher before 30 min p.i. as could be seen in the Experimental Section where radioactivity accumulation in the tumor was quantified from the U-SPECT images of ^{99m}Tc-HABN. High tumor-to-background ratios were obtained due to low uptake of radioactivity in bone and muscle on one hand and the rapid clearance from the blood pool on the other hand. Generally, T/NT ratios increased over time because of the long retention time of the radiotracer in tumor, confirming the *in vitro* results of the efflux experiment. As was expected, high uptake was detected in the GRPR rich mouse pancreas,[34] but was reduced significantly ($p < 0.0001$) when the blocking agent HYNIC-Aca-BN(7−14) was injected prior to injection of ^{99m}Tc-HABN. Uptake in tumor, stomach, and intestine was also significantly reduced in the study of GRPR blockade, indicating that uptake was also GRPR mediated.

At first glance the tumor uptake appears rather low when compared to the best performing BN analogues reported in the literature. However, when the best performing BN analogues demobesin-1 (reported % ID/g ranging from 13.45 to 24.61[40,44,45]), DOTA-PESIN (14.8% ID/g[41]) and AMBA (6.35% ID/g[39]) were compared under the same circumstances in a study by Schroeder et al., uptake by PC-3 xenografts 1 h p.i. was considerably lower and not statistically significantly different from each other (3.0, 2.3 and 2.7% ID/g, respectively).[46] Furthermore, the results of Schroeder et al. are not so different from the results reported by other authors or our results.[17] Schroeder stated that the variation in radionuclides, amounts of peptide, mouse strain (species, sex, weight), PC-3 cells used (passage number, culture conditions), tumor size and vascularization of the tumor may all be factors that determine uptake of radioactivity in tumor resulting in variable outcomes.[46]

As can be appreciated from our microSPECT images, there is high uptake of activity in the outer tumor regions resulting in a "hot rim" around a central area with lower uptake. As several authors have shown before, the central part of a xenograft tumor is often necrotic or prenecrotic with reduced viable cell density, especially in larger tumors, which can result in lower central uptake of a radiotracer.[46−48] When measuring total tumor uptake of a radiotracer, the central necrosis, reduced central cell viability and reduced vascularization or diffusion will result in an underestimation of the actual tumor cell uptake. Even with standardization of the different variables mentioned by Schroeder et al., because of these many variables influencing the outcome of the experiments, a comparison between individual radiopharmaceuticals tested in separate studies is in fact rather difficult.

Absolute tumor uptake is an important factor, but for good image contrast high T/NT ratios are also imperative. Rapid internalization observed *in vitro* (70−80% within 5−15 min) is reflected in rapid tumor uptake in mice, which can be appreciated from the microSPECT images as activity is already appearing in the first time frame after 10 min. However, because uptake in other organs is also rapid in combination with high circulating levels of activity in the blood, the tumor-to-background contrast after 10 min is rather low. Still, the tumor is clearly visualized after 10 min and even better after 20 min or more. While internalization was quick, PC-3 cell efflux was slow both *in vitro* and *in vivo*, with persistent retention of activity in the tumor resulting in increasing T/NT ratios and clear delineation of the tumor over time up to 4 h p.i.

Multiple BN-like radiopharmaceuticals with many different designs have been shown to be highly specific for GRPR and sensitive for prostate cancer. So far, studies on antagonists that have been recently published have mostly shown higher or at least similar tumor uptake and T/NT ratios when compared to agonist compounds.[42,49−52] However, in the previously mentioned study by Schroeder et al. multiple BN-agonists were compared to an antagonist and, although the latter showed the highest uptake in tumor, this was not significant.[46] Despite these contrasting results, it will be interesting to see how these preclinical studies will translate into clinical studies as there may be large interspecies differences between mice and men with respect to GRPR imaging. For example, in humans, differences in metabolism, excretion, nontarget GRPR expression, prostate tumor characteristics, vascularization or anatomy may account for uptake differences. Also, background interference from bladder or intestinal tissues may or may not hinder detection of (extra)-prostatic cancer foci or lymph node metastases.

For clinical imaging purposes, small tumors pose a diagnostic dilemma as they cannot be detected by conventional imaging techniques like CT or MRI, because these techniques have a limited resolution and depend on morphology (size and shape criteria) for making a diagnosis. SPECT and PET can be superior techniques as they may be able to differentiate between benign or malignant tissue based on differences in metabolism and contrast (e.g., T/NT ratios), rather than on morphology.

In conclusion ^{99m}Tc-HABN is a novel BN-based radiopharmaceutical that proved to be suitable for targeted imaging of prostate cancer using microSPECT in a human derived PC-3 xenograft model.

AUTHOR INFORMATION

Corresponding Author

*Hanzeplein 1, 9712 RB Groningen, The Netherlands. E-mail: h.j.k.ananias@uro.umcg.nl. Phone: 0031503612380. Fax: 0031503619607.

ACKNOWLEDGMENT

We thank Jurgen Sijbesma for his assistance with the animal experiments and Chao Wu for his assistance with the microSPECT imaging and image reconstruction. This work was supported by grants of the Dutch Cancer Society (KWF 2008-4243), the Dutch Urology Foundation 1973 (Stichting Urologie 1973) and the Jan Kornelis de Cock Stichting (J.K. de Cock Stichting 08-02).

ABBREVIATIONS USED

SPECT, single photon emission computed tomography; PET, positron emission tomography; GRPR, gastrin-releasing peptide receptor; GRP, gastrin-releasing peptide; BN, bombesin; ^{99m}Tc-HABN, ^{99m}Tc-HYNIC(tricine/TPPTS)-Aca-BN(7−14); TPPTS, trisodium triphenylphosphine-3,3′,3″-trisulfonate; p.i., postinjection; % ID/g, percentage of the injected dose per gram of tissue mass; Aca, ε-aminocaproic acid; HYNIC, 6-hydrazinonicotinic acid; T/NT, tumor-to-normal-tissue; CT, computed tomography; SPECT, single photon emission computed tomography; SD, standard deviation; IC_{50}, 50% inhibitory concentration; RCP, radiochemical purity; ROI, region of interest; Boc, *tert*-butyloxycarbonyl

REFERENCES

(1) Jemal, A.; Siegel, R.; Ward, E.; Hao, Y.; Xu, J.; Thun, M. J. Cancer statistics, 2009. *CA—Cancer J. Clin.* **2009**, *59*, 225–249.

(2) Ferlay, J.; Parkin, D. M.; Steliarova-Foucher, E. Estimates of cancer incidence and mortality in Europe in 2008. *Eur. J. Cancer* **2010**, *46*, 765–781.

(3) Albertsen, P. C.; Hanley, J. A.; Harlan, L. C.; Gilliland, F. D.; Hamilton, A.; Liff, J. M.; Stanford, J. L.; Stephenson, R. A. The positive yield of imaging studies in the evaluation of men with newly diagnosed prostate cancer: a population based analysis. *J. Urol.* **2000**, *163*, 1138–1143.

(4) Hovels, A. M.; Heesakkers, R. A.; Adang, E. M.; Jager, G. J.; Strum, S.; Hoogeveen, Y. L.; Severens, J. L.; Barentsz, J. O. The diagnostic accuracy of CT and MRI in the staging of pelvic lymph nodes in patients with prostate cancer: a meta-analysis. *Clin. Radiol.* **2008**, *63*, 387–395.

(5) Zaheer, A.; Cho, S. Y.; Pomper, M. G. New agents and techniques for imaging prostate cancer. *J. Nucl. Med.* **2009**, *50*, 1387–1390.

(6) Picchio, M.; Giovannini, E.; Messa, C. The role of PET/computed tomography scan in the management of prostate cancer. *Curr. Opin. Urol.* **2011**, *21*, 230–236.

(7) Hong, H.; Zhang, Y.; Sun, J.; Cai, W. Positron emission tomography imaging of prostate cancer. *Amino Acids* **2010**, *39*, 11–27.

(8) Beheshti, M.; Langsteger, W.; Fogelman, I. Prostate cancer: role of SPECT and PET in imaging bone metastases. *Semin. Nucl. Med.* **2009**, *39*, 396–407.

(9) Ananias, H. J.; van den Heuvel, M. C.; Helfrich, W.; de Jong, I. J. Expression of the gastrin-releasing peptide receptor, the prostate stem cell antigen and the prostate-specific membrane antigen in lymph node and bone metastases of prostate cancer. *Prostate* **2009**, *69*, 1101–1108.

(10) Markwalder, R.; Reubi, J. C. Gastrin-releasing peptide receptors in the human prostate: relation to neoplastic transformation. *Cancer Res.* **1999**, *59*, 1152–1159.

(11) Reubi, J. C.; Wenger, S.; Schmuckli-Maurer, J.; Schaer, J. C.; Gugger, M. Bombesin receptor subtypes in human cancers: detection with the universal radioligand (125)I-[D-TYR(6), beta-ALA(11), PHE-(13), NLE(14)] bombesin(6−14). *Clin. Cancer Res.* **2002**, *8*, 1139–1146.

(12) Waser, B.; Eltschinger, V.; Linder, K.; Nunn, A.; Reubi, J. C. Selective in vitro targeting of GRP and NMB receptors in human tumours with the new bombesin tracer 177Lu-AMBA. *Eur. J. Nucl. Med. Mol. Imaging* **2007**, *34*, 95–100.

(13) Aprikian, A. G.; Cordon-Cardo, C.; Fair, W. R.; Reuter, V. E. Characterization of neuroendocrine differentiation in human benign prostate and prostatic adenocarcinoma. *Cancer* **1993**, *71*, 3952–3965.

(14) Cutz, E.; Chan, W.; Track, N. S. Bombesin, calcitonin and leu-enkephalin immunoreactivity in endocrine cells of human lung. *Experientia* **1981**, *37*, 765–767.

(15) Price, J.; Penman, E.; Wass, J. A.; Rees, L. H. Bombesin-like immunoreactivity in human gastrointestinal tract. *Regul. Pept.* **1984**, *9*, 1–10.

(16) Spindel, E. R.; Chin, W. W.; Price, J.; Rees, L. H.; Besser, G. M.; Habener, J. F. Cloning and characterization of cDNAs encoding human gastrin-releasing peptide. *Proc. Natl. Acad. Sci. U.S.A.* **1984**, *81*, 5699–5703.

(17) Ananias, H. J.; de Jong, I. J.; Dierckx, R. A.; Van de Wiele, C.; Helfrich, W.; Elsinga, P. H. Nuclear imaging of prostate cancer with gastrin-releasing-peptide-receptor targeted radiopharmaceuticals. *Curr. Pharm. Des* **2008**, *14*, 3033–3047.

(18) Hohla, F.; Schally, A. V. Targeting gastrin releasing peptide receptors: New options for the therapy and diagnosis of cancer. *Cell Cycle* **2010**, *9*, 1738–1741.

(19) Schroeder, R. P.; van Weerden, W. M.; Bangma, C.; Krenning, E. P.; de, J. M. Peptide receptor imaging of prostate cancer with radiolabelled bombesin analogues. *Methods* **2009**, *48*, 200–204.

(20) De Vincentis, G.; Scopinaro, F.; Varvarigou, A.; Ussof, W.; Schillaci, O.; Archimandritis, S.; Corleto, V.; Longo, F.; Delle, F. G. Phase I trial of technetium [Leu13] bombesin as cancer seeking agent: possible scintigraphic guide for surgery?. *Tumori* **2002**, *88*, S28–S30.

(21) De Vincentis, G.; Remediani, S.; Varvarigou, A. D.; Di Santo., G.; Iori, F.; Laurenti, C.; Scopinaro, F. Role of 99mTc-bombesin scan in diagnosis and staging of prostate cancer. *Cancer Biother. Radiopharm.* **2004**, *19*, 81–84.

(22) Scopinaro, F.; De Vincentis, G.; Varvarigou, A. D.; Laurenti, C.; Iori, F.; Remediani, S.; Chiarini, S.; Stella, S. 99mTc-bombesin detects prostate cancer and invasion of pelvic lymph nodes. *Eur. J. Nucl. Med. Mol. Imaging* **2003**, *30*, 1378–1382.

(23) Van de Wiele, C.; Dumont, F.; Vanden Broecke, R.; Oosterlinck, W.; Cocquyt, V.; Serreyn, R.; Peers, S.; Thornback, J.; Slegers, G.; Dierckx, R. A. Technetium-99m RP527, a GRP analogue for visualisation of GRP receptor-expressing malignancies: a feasibility study. *Eur. J. Nucl. Med.* **2000**, *27*, 1694–1699.

(24) Van de Wiele, C.; Dumont, F.; Dierckx, R. A.; Peers, S. H.; Thornback, J. R.; Slegers, G.; Thierens, H. Biodistribution and dosimetry of (99m)Tc-RP527, a gastrin-releasing peptide (GRP) agonist for the visualization of GRP receptor-expressing malignancies. *J. Nucl. Med.* **2001**, *42*, 1722–1727.

(25) Liu, S.; Edwards, D. S. 99mTc-Labeled Small Peptides as Diagnostic Radiopharmaceuticals. *Chem. Rev.* **1999**, *99*, 2235–2268.

(26) Wang, L.; Shi, J.; Kim, Y. S.; Zhai, S.; Jia, B.; Zhao, H.; Liu, Z.; Wang, F.; Chen, X.; Liu, S. Improving tumor-targeting capability and pharmacokinetics of (99m)Tc-labeled cyclic RGD dimers with PEG(4) linkers. *Mol. Pharmaceutics* **2009**, *6*, 231–245.

(27) Liu, S.; Harris, A. R.; Williams, N. E.; Edwards, D. S. 99mTc-Labeling of a hydrazinonicotinamide-conjugated LTB(4) receptor antagonist useful for imaging infection and inflammation. *Bioconjugate Chem.* **2002**, *13*, 881–886.

(28) Edwards, D. S.; Liu, S.; Barrett, J. A.; Harris, A. R.; Looby, R. J.; Ziegler, M. C.; Heminway, S. J.; Carroll, T. R. New and versatile ternary ligand system for technetium radiopharmaceuticals: water soluble phosphines and tricine as coligands in labeling a hydrazinonicotinamide-modified cyclic glycoprotein IIb/IIIa receptor antagonist with 99mTc. *Bioconjugate Chem.* **1997**, *8*, 146–154.

(29) Shi, J.; Jia, B.; Liu, Z.; Yang, Z.; Yu, Z.; Chen, K.; Chen, X.; Liu, S.; Wang, F. (99m)Tc-Labeled Bombesin(7−14)NH2 with Favorable Properties for SPECT Imaging of Colon Cancer. *Bioconjugate Chem.* **2008**, *19*, 1170–1178.

(30) Guo, H.; Xie, F.; Zhu, M.; Li, Y.; Yang, Z.; Wang, X.; Lu, J. The synthesis of pteroyl-lys conjugates and its application as Technetium-99m labeled radiotracer for folate receptor-positive tumor targeting. *Bioorg. Med. Chem. Lett.* **2011**, *21*, 2025–2029.

(31) Lu, J.; Pang, Y.; Xie, F.; Guo, H.; Li, Y.; Yang, Z.; Wang, X. Synthesis and in vitro/in vivo evaluation of (99m)Tc-labeled folate conjugates for folate receptor imaging. *Nucl. Med. Biol.* **2011**, *38*, 557–565.

(32) Zhang, X.; Cai, W.; Cao, F.; Schreibmann, E.; Wu, Y.; Wu, J. C.; Xing, L.; Chen, X. 18F-labeled bombesin analogs for targeting GRP receptor-expressing prostate cancer. *J. Nucl. Med.* **2006**, *47*, 492–501.

(33) Chen, X.; Park, R.; Hou, Y.; Tohme, M.; Shahinian, A. H.; Bading, J. R.; Conti, P. S. microPET and autoradiographic imaging of GRP receptor expression with 64Cu-DOTA-[Lys3]bombesin in human prostate adenocarcinoma xenografts. *J. Nucl. Med.* **2004**, *45*, 1390–1397.

(34) Fanger, B. O.; Wade, A. C.; Cardin, A. D. Characterization of the murine pancreatic receptor for gastrin releasing peptide and bombesin. *Regul. Pept.* **1991**, *32*, 241–251.

(35) Faintuch, B. L.; Teodoro, R.; Duatti, A.; Muramoto, E.; Faintuch, S.; Smith, C. J. Radiolabeled bombesin analogs for prostate cancer diagnosis: preclinical studies. *Nucl. Med. Biol.* **2008**, *35*, 401–411.

(36) Santos-Cuevas, C. L.; Ferro-Flores, G.; Arteaga de, M. C.; Pichardo-Romero, P. A. Targeted imaging of gastrin-releasing peptide receptors with 99mTc-EDDA/HYNIC-[Lys3]-bombesin: biokinetics and dosimetry in women. *Nucl. Med. Commun.* **2008**, *29*, 741–747.

(37) Garcia-Garayoa, E.; Schweinsberg, C.; Maes, V.; Ruegg, D.; Blanc, A.; Blauenstein, P.; Tourwe, D. A.; Beck-Sickinger, A. G.; Schubiger, P. A. New [99mTc]bombesin analogues with improved biodistribution for targeting gastrin releasing-peptide receptor-positive tumors. *Q. J. Nucl. Med. Mol. Imaging* **2007**, *51*, 42–50.

(38) Garcia-Garayoa, E.; Ruegg, D.; Blauenstein, P.; Zwimpfer, M.; Khan, I. U.; Maes, V.; Blanc, A.; Beck-Sickinger, A. G.; Tourwe, D. A.;

Schubiger, P. A. Chemical and biological characterization of new Re(CO)3/[99mTc](CO)3 bombesin analogues. *Nucl. Med. Biol.* **2007**, *34*, 17–28.

(39) Lantry, L. E.; Cappelletti, E.; Maddalena, M. E.; Fox, J. S.; Feng, W.; Chen, J.; Thomas, R.; Eaton, S. M.; Bogdan, N. J.; Arunachalam, T.; Reubi, J. C.; Raju, N.; Metcalfe, E. C.; Lattuada, L.; Linder, K. E.; Swenson, R. E.; Tweedle, M. F.; Nunn, A. D. 177Lu-AMBA: Synthesis and characterization of a selective 177Lu-labeled GRP-R agonist for systemic radiotherapy of prostate cancer. *J. Nucl. Med.* **2006**, *47*, 1144–1152.

(40) Maina, T.; Nock, B. A.; Zhang, H.; Nikolopoulou, A.; Waser, B.; Reubi, J. C.; Maecke, H. R. Species differences of bombesin analog interactions with GRP-R define the choice of animal models in the development of GRP-R-targeting drugs. *J. Nucl. Med.* **2005**, *46*, 823–830.

(41) Zhang, H.; Schuhmacher, J.; Waser, B.; Wild, D.; Eisenhut, M.; Reubi, J. C.; Maecke, H. R. DOTA-PESIN, a DOTA-conjugated bombesin derivative designed for the imaging and targeted radionuclide treatment of bombesin receptor-positive tumours. *Eur. J. Nucl. Med. Mol. Imaging* **2007**, *34*, 1198–1208.

(42) Mansi, R.; Wang, X.; Forrer, F.; Waser, B.; Cescato, R.; Graham, K.; Borkowski, S.; Reubi, J. C.; Maecke, H. R. Development of a potent DOTA-conjugated bombesin antagonist for targeting GRPr-positive tumours. *Eur. J. Nucl. Med. Mol. Imaging* **2011**, *38*, 97–107.

(43) Koumarianou, E.; Mikolajczak, R.; Pawlak, D.; Zikos, X.; Bouziotis, P.; Garnuszek, P.; Karczmarczyk, U.; Maurin, M.; Archimandritis, S. C. Comparative study on DOTA-derivatized bombesin analog labeled with 90Y and 177Lu: in vitro and in vivo evaluation. *Nucl. Med. Biol.* **2009**, *36*, 591–603.

(44) Nock, B.; Nikolopoulou, A.; Chiotellis, E.; Loudos, G.; Maintas, D.; Reubi, J. C.; Maina, T. [99mTc]Demobesin 1, a novel potent bombesin analogue for GRP receptor-targeted tumour imaging. *Eur. J. Nucl. Med. Mol. Imaging* **2003**, *30*, 247–258.

(45) Cescato, R.; Maina, T.; Nock, B.; Nikolopoulou, A.; Charalambidis, D.; Piccand, V.; Reubi, J. C. Bombesin receptor antagonists may be preferable to agonists for tumor targeting. *J. Nucl. Med.* **2008**, *49*, 318–326.

(46) Schroeder, R. P.; Muller, C.; Reneman, S.; Melis, M. L.; Breeman, W. A.; de, B. E.; Bangma, C. H.; Krenning, E. P.; van Weerden, W. M.; de, J. M. A standardised study to compare prostate cancer targeting efficacy of five radiolabelled bombesin analogues. *Eur. J. Nucl. Med. Mol. Imaging* **2010**, *37*, 1386–1396.

(47) Dearling, J. L.; Flynn, A. A.; Sutcliffe-Goulden, J.; Petrie, I. A.; Boden, R.; Green, A. J.; Boxer, G. M.; Begent, R. H.; Pedley, R. B. Analysis of the regional uptake of radiolabeled deoxyglucose analogs in human tumor xenografts. *J. Nucl. Med.* **2004**, *45*, 101–107.

(48) Bao, A.; Phillips, W. T.; Goins, B.; McGuff, H. S.; Zheng, X.; Woolley, F. R.; Natarajan, M.; Santoyo, C.; Miller, F. R.; Otto, R. A. Setup and characterization of a human head and neck squamous cell carcinoma xenograft model in nude rats. *Otolaryngol. Head Neck Surg.* **2006**, *135*, 853–857.

(49) Honer, M.; Mu, L.; Stellfeld, T.; Graham, K.; Martic, M.; Fischer, C. R.; Lehmann, L.; Schubiger, P. A.; Ametamey, S. M.; Dinkelborg, L.; Srinivasan, A.; Borkowski, S. 18F-labeled bombesin analog for specific and effective targeting of prostate tumors expressing gastrin-releasing peptide receptors. *J. Nucl. Med.* **2011**, *52*, 270–278.

(50) Lane, S. R.; Nanda, P.; Rold, T. L.; Sieckman, G. L.; Figueroa, S. D.; Hoffman, T. J.; Jurisson, S. S.; Smith, C. J. Optimization, biological evaluation and microPET imaging of copper-64-labeled bombesin agonists, [64Cu-NO2A-(X)-BBN(7−14)NH2], in a prostate tumor xenografted mouse model. *Nucl. Med. Biol.* **2010**, *37*, 751–761.

(51) Mansi, R.; Wang, X.; Forrer, F.; Kneifel, S.; Tamma, M. L.; Waser, B.; Cescato, R.; Reubi, J. C.; Maecke, H. R. Evaluation of a 1,4,7,10-tetraazacyclododecane-1,4,7,10-tetraacetic acid-conjugated bombesin-based radioantagonist for the labeling with single-photon emission computed tomography, positron emission tomography, and therapeutic radionuclides. *Clin. Cancer Res.* **2009**, *15*, 5240–5249.

(52) Lears, K. A.; Ferdani, R.; Liang, K.; Zheleznyak, A.; Andrews, R.; Sherman, C. D.; Achilefu, S.; Anderson, C. J.; Rogers, B. E. In vitro and in vivo evaluation of 64Cu-labeled SarAr-bombesin analogs in gastrin-releasing peptide receptor-expressing prostate cancer. *J. Nucl. Med.* **2011**, *52*, 470–477.

(53) Surfraz, M. B.; King, R.; Mather, S. J.; Biagini, S.; Blower, P. J. Technetium-binding in labelled HYNIC-peptide conjugates: role of coordinating amino acids. *J. Inorg. Biochem.* **2009**, *103*, 971–977.